Spectrochimica Acta Part B 66 (2011) 179–185

Contents lists available at ScienceDirect

Spectrochimica Acta Part B

journal homepage: www.elsevier.com/locate/sab

Research Note

The influence of laser-particle interaction in laser induced breakdown spectroscopy and laser ablation inductively coupled plasma spectrometry[1]

Helmut Lindner [a], Kristofer H. Loper [b], David W. Hahn [b], Kay Niemax [c,*]

[a] Department of Chemistry Research Group for Plasma, Laser Ablation and Surface Modeling-Antwerp (PLASMANT), University of Antwerp, Universiteitsplein 1, B-2610 Wilrijk, Belgium
[b] Department of Mechanical & Aerospace Engineering, University of Florida, Gainesville, FL, USA
[c] Department of Analytical Chemistry and Reference Materials, Federal Institute for Materials Research and Testing (BAM), Richard-Willstätter-Strasse 11, 12489 Berlin, Germany

ARTICLE INFO

Article history:
Received 21 September 2010
Accepted 12 January 2011
Available online 19 January 2011

Keywords:
Laser-particle interaction
LIBS
LA-ICP spectrometry

ABSTRACT

Particles produced by previous laser shots may have significant influence on the analytical signal in laser-induced breakdown spectroscopy (LIBS) and laser ablation inductively coupled plasma (LA-ICP) spectrometry if they remain close to the position of laser sampling. The effects of these particles on the laser-induced breakdown event are demonstrated in several ways. LIBS-experiments were conducted in an ablation cell at atmospheric conditions in argon or air applying a dual-pulse arrangement with orthogonal pre-pulse, i.e., plasma breakdown in a gas generated by a focussed laser beam parallel and close to the sample surface followed by a delayed crossing laser pulse in orthogonal direction which actually ablates material from the sample and produces the LIBS plasma. The optical emission of the LIBS plasma as well as the absorption of the pre-pulse laser was measured. In the presence of particles in the focus of the pre-pulse laser, the plasma breakdown is affected and more energy of the pre-pulse laser is absorbed than without particles. As a result, the analyte line emission from the LIBS plasma of the second laser is enhanced. It is assumed that the enhancement is not only due to an increase of mass ablated by the second laser but also to better atomization and excitation conditions favored by a reduced gas density in the pre-pulse plasma. Higher laser pulse frequencies increase the probability of particle-laser interaction and, therefore, reduce the shot-to-shot line intensity variation as compared to lower particle loadings in the cell. Additional experiments using an aerosol chamber were performed to further quantify the laser absorption by the plasma in dependence on time both with and without the presence of particles. The overall implication of laser-particle interactions for LIBS and LA-ICP-MS/OES are discussed.

1. Introduction

One of the crucial pre-conditions in all analytical methods with sampling by pulsed laser radiation is the reproducible delivery of the laser energy to the surface of the sample. Variations of the laser fluence from shot to shot will not only affect the interaction of the laser with the sample, e.g., by removing different masses, but also the physical conditions in the plasma formed by the breakdown on the surface. The highly non-linear nature of pulsed laser material interactions serves to enhance such non-linearities. While the influence of varying laser fluence on laser sampling is generally accepted, and lasers with high pulse reproducibility are preferred, the influence of particles near the laser focus which may modify the plasma breakdown and the analyte sampling process is often neglected. It is well-known that particles can seed a breakdown (i.e., effectively lower the breakdown threshold up to several orders of magnitude) in gas where no plasma would be generated without a particle [1–5]. However, laser-particle interaction has also an impact on the physical plasma conditions if the fluence of the laser is so large that there is plasma breakdown in a gas without particles [6,7]. Such particle induced breakdown very near to the surface will absorb energy from the incident laser pulse delivered to the surface, and, therefore, have influence on the laser ablation process from a solid sample and, for example, also on the emission spectra in a LIBS experiment. The influence of particles on the ablation process has been discussed recently in [8], but not shown explicitly.

In the present paper laser-particle interaction is decoupled from the LIBS process and the fluence of the first laser is so large that there is plasma breakdown in the gas also without particles in the focus. The decoupling of the two processes is achieved using the so-called double-pulse arrangement with orthogonal pre-pulse [9–17], in which the first laser beam, oriented parallel and close to the sample surface, is focused just above the position where a second, orthogonal (i.e. perpendicular to the target surface) laser beam is producing the

* Corresponding author.
E-mail address: kay.niemax@bam.de (K. Niemax).

[1] Research has been performed within the network Plasma-Analyte Interaction Working Group (PAIWG). PAIWG is a collaborative effort of the University of Florida (Gainesville, USA) and the Federal Institute for Materials Research and Testing (BAM, Berlin, Germany), jointly funded by NSF and DFG.

0584-8547/$ – see front matter © 2011 Elsevier B.V. All rights reserved.
doi:10.1016/j.sab.2011.01.002

LIBS plasma with a specified time-delay. It will be shown that the presence of particles in the pre-pulse plasma have a significant enhancement effect on the emission line intensities of the delayed LIBS process and on the reproducibility of the LIBS spectra.

Complementary experiments were performed with a single laser using an aerosol chamber for laser-induced breakdown directly in the aerosol stream, allowing direct assessment of the plasma absorption and shot-to-shot statistics for defined aerosol loadings.

2. Experiment

Two specific experimental platforms were used in the current study. The first experimental arrangement is basically the same as reported in [14,18]. Two Nd:YAG lasers (1064-nm wavelength; ~8-ns pulse width) were applied for orthogonal pre-pulse ablation in a cylindrical cell (30-mm diameter; 17 cm^3 volume) as shown in Fig. 1. The cell was equipped with three quartz windows, one on top of the cell opposite to the sample for the ablation beam, and on two opposite side walls for the pre-pulse laser beam to enter and exit. Ablation was performed either in high-purity argon or in ambient air both at atmospheric pressure. The ambient air was not filtered. Thus, laboratory dust particles of unknown concentration were introduced with the air into the ablation cell. The ablation laser was a Nd:YAG operating at 10 mJ per pulse. The pre-pulse Nd:YAG laser had an additional amplifier stage and was operated at 91 mJ per pulse, which was sufficient for direct breakdown of air or argon. A fixed time delay of 20 μs was used between the pre-pulse and ablation pulse lasers, and was controlled using a pulse delay generator (Stanford Research DG 535). The beam of the pre-pulse laser was focussed by a 61.5-mm lens through one of the side windows at a height of 2.5 mm above the ablation target surface. The beam of the ablation laser was focussed through a pierced mirror by a 100-mm lens such that the focal point was 1.5 mm below the polished surface of a standard brass sample (60.6% Cu, 39.4% Zn). The set-up produced a beam diameter of about 75 μm on the target surface. Taking into account the power of the ablation laser and the diameter of the Gaussian laser beam, the peak fluence on the surface was about 460 J cm^{-2}.

In order not to produce deep craters and to change the particle size distribution too much, only 300 shots were applied to each spot before the sample was shifted. For this study, the inner crater diameters were measured with a scanning electron microscope, yielding values of about 130 μm after 300 shots. The laser pulse frequency was varied in the range of 0.1–5 Hz. The ablation particles

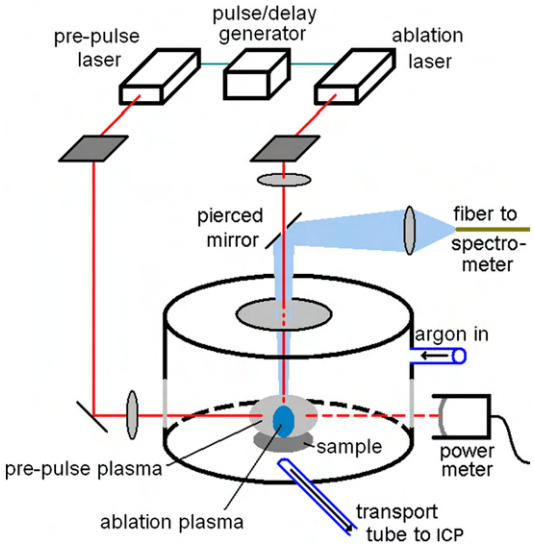

Fig. 1. Experimental arrangement for dual-pulse LIBS with orthogonal pre-pulse, absorption measurements of the pre-pulse energy, and ICP-OES.

produced were transported through a 4 mm wide PVC-tube to the torch of a prototype ICP-instrument (ELEMENT 1, Finnigan MAT, Bremen, Germany).

The RF-generator (27 MHz) for the ICP and the matching unit (AM/ICP-20P) were provided by RF Power Products Inc. (Marlton, NJ). The ICP power was 800 W while the sample gas flow through the ablation cell and ICP-injector tube was 0.3 L/min. The flows of the plasma gas and the auxiliary gas in the ICP were 18 and 2 L/min, respectively.

The end-on emission of the ICP was focussed by a 10-cm quartz lens into a quartz bundle fiber with a core diameter of 4 mm. It was assured that the total relevant volume of the plasma where atomization of the particles is occurring was imaged onto the fiber-core. The fiber split into two identical fibers, leading the emission to two different monochromators (not shown in Fig. 1). One was a Spex 1000 M (1-m focal length; 1200-grooves/mm grating) and the other a custom 0.45-m Czerny-Turner mount monochromator with 1200 grooves/mm grating. The radiations from the fibers were collimated by quartz optics to match the numerical apertures of the respective monochromator. One monochromator was set to an atomic zinc line (213.8 nm, 330.3 nm, or 334.5 nm), and the other to the atomic copper line at 324.8 nm. In this way, the brass constituents, namely copper and zinc, could be measured simultaneously using fast photomultiplier tubes (EMI type 9789 QA, rise time: 10 ns) on each monochromator. For acquiring the data an A/D converter was used. The data uptake rate was set to 2000/s.

The emission from the LIBS plasma for this platform was measured by collecting the radiation using the pierced mirror and imaging it directly onto the fiber, as shown in Fig. 1. The spectra were measured by an Échelle-spectrometer (ESA 3000 by LLA, Berlin) equipped with an intensified charge-coupled device (ICCD). The delay and integration times were 3 μs and 10 μs, respectively, after the ablation pulse.

The transmission of the pre-pulse laser beam through the plasma produced in the gas above the sample was measured with a bolometer (Oriel, Type: C120) which, due to its slow response, recorded the integral transmission. The incident laser power was measured with a defocused laser beam avoiding a plasma breakdown.

The second experimental platform used a single laser for breakdown directly in an aerosol sample chamber. Specifically, laser-induced breakdown measurements were recorded in a 6-way cross for HEPA-filtered pure nitrogen gas flow (10 L/min), and for an aerosol flow of sodium chloride nanoparticles. A Nd:YAG laser operated at 1064 nm (100 mJ/pulse, 10-ns fwhm) was used to create the plasma in the center of the cross using a 100-mm plano-convex lens. This LIBS system was reported previously [7]. UV-grade quartz windows allowed the laser beam to enter and exit the sample cross. The transmitted laser pulse was recorded using a fast-response phototube (200-ps rise time) and recorded using a digitizing oscilloscope (500 MHz and 4 Gs/s). To minimize plasma emission on the phototube, the exiting beam was turned 90° using a quartz flat and then another 90° using a 1064-nm dichroic mirror. Neutral density filters were used as necessary to reduce the signal level to well within the linear response range for all measurements.

The aerosol was created with a pneumatic nebulizer (TSI 3076) using a dilute solution of sodium chloride in ultrapurified water. The nebulizer output stream was immediately mixed with a 10 L/min co-flow of HEPA-filtered, dry nitrogen in a mixing chamber, and then passed through a desiccant diffusion dryer prior to entering the LIBS sample chamber. Solution concentrations of sodium chloride were selected to produce dry nanoparticles with a geometric mean diameter of 50 or 75 nm following desolvation, per the manufacturer's specifications. Particle counts were measured in the sample chamber for the two different size distributions using a light-scattering based particle counter with a sensitivity range from 100 nm to 2 μm. Manufacturer particle size distribution specifications for sodium chloride nebulization were then used to calculate the total particle counts based on the counts directly measured over the 100 nm to

2 μm size range, which directly recorded just over 50% of the total particle counts.

3. Results and discussion

The top of Fig. 2 shows 20 individual dual-pulse LIBS spectra measured after the respective ablation pulses at very low laser frequency (0.1 Hz). The line intensities are observed to fluctuate significantly. To more clearly demonstrate the fluctuation and show the possible intensity correlation of the Zn and Cu lines, the bottom of Fig. 2 displays a selection of six spectra from the top figure. The peak intensities of the Zn and Cu lines of Fig. 2 and their ratios are plotted in Fig. 3 for all 20 shots. While the relative standard deviations (RSD) of the Zn and Cu intensities are large (57% and 58%, respectively), the RSD of their ratios is only 15%. This indicates a correlation between the Zn and Cu line intensities. The variations are due to the statistical presence of particles in the focus region of the pre-pulse, as will be shown below. It should be mentioned here that the line intensity scatter became smaller at larger pulse frequency. For example, the line intensity scatter reached RSD values of about 15% at 5 Hz, which is on the order of RSD data published in literature [9–13].

Recently, it was demonstrated that the mass ablated in a double-pulse arrangement with orthogonal pre-pulse is dependent on the energy of the pre-pulse if the power of the ablation pulse is constant [14]. As observed, the higher the pre-pulse laser energy, the larger is the mass ablated. In first approximation, the dependence appeared linear.

The hypothesis here is that the energy absorbed by the pre-pulse laser is higher in the presence of particles as compared to particle-free

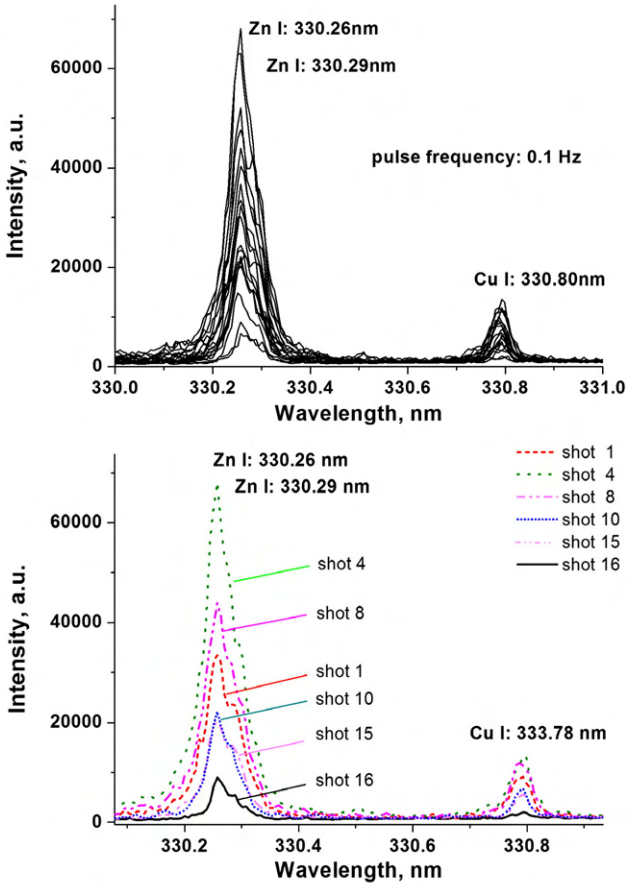

Fig. 2. Intensity fluctuation of successive dual-pulse LIBS spectra of brass measured at a laser pulse frequency of 0.1 Hz. (top figure) 20 individual spectra; (bottom figure) a choice of six spectra out of 20 shown in top figure.

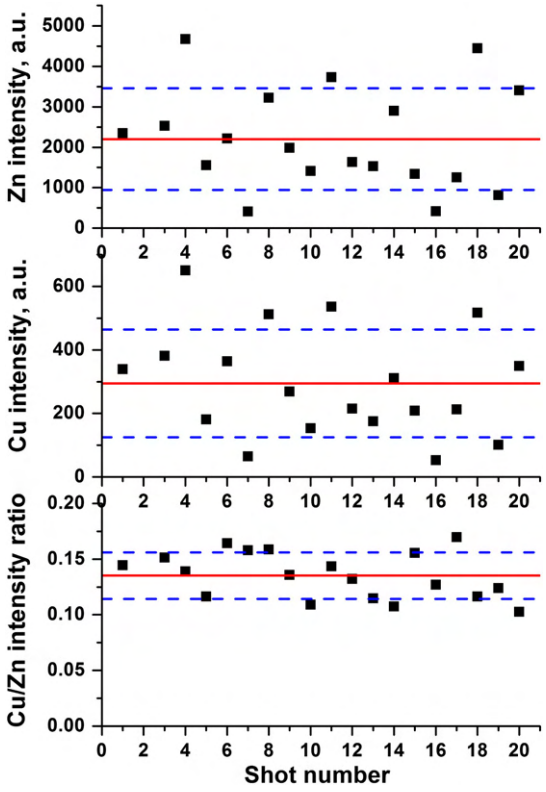

Fig. 3. The Zn and Cu line peak intensities of the 20 single spectra of Fig. 1 and their ratios. The full lines represent the average values while the dashed lines show the relative standard deviations: 57%, 58%, and 15% for Zn, Cu and the Cu/Zn ratio, respectively.

gas, and, therefore, more mass is sampled by the ablation laser. However, also the atomization and excitation conditions are improved because the enhancement of the spectra in comparison with pre-pulse breakdown without particles is larger than the increment of mass ablated. We will see later in time-resolved transmission measurements using the second platform that plasma breakdown occurs slightly earlier with laser-particle interaction and, therefore, more energy is absorbed from the laser pulse. More absorbed energy means hotter pre-pulse plasmas with lower gas densities in the shock-wave bubble than without particles. The intensities of LIBS spectra are known to be strongly dependent on the pressure, i.e., the number density, of the surrounding gas (see, e.g., [19,20]).

The influence of particles on the absorbed energy from the first laser can be investigated measuring its transmission through the pre-pulse plasma. This is first done for the ablation cell using the first platform, and then repeated with high time resolution in the more controlled aerosol sample chamber using the second platform.

The transmission measurements were made at various pulse frequencies with a constant Ar gas flow of 0.3 L/min in order to wash the particles out of the cell, i.e., to change the probability of having particles in the focus region of the pre-pulse laser. The presence of particles in the ablation cell and the magnitude of particle loading were measured by ICP-OES. For example, Fig. 4 shows the transmissions measured at 0.6 and 5 Hz together with the ICP-OES signals of the Zn 213.8 nm line shown the presence of brass particles in the ablation cell. Before the ablation laser started sampling, the transmission was about 14% with relative small data scatter from shot-to-shot. As can be seen from the ICP-OES signal, at that time there were almost no particles in the cell. The few which are recorded are from an earlier ablation process before. When sampling started at 45 s for the 0.6 Hz case, the transmission decreased to an average value of about 11%; however, with significant shot-to-shot scatter. Ablation was stopped after 90 s, and the average transmission

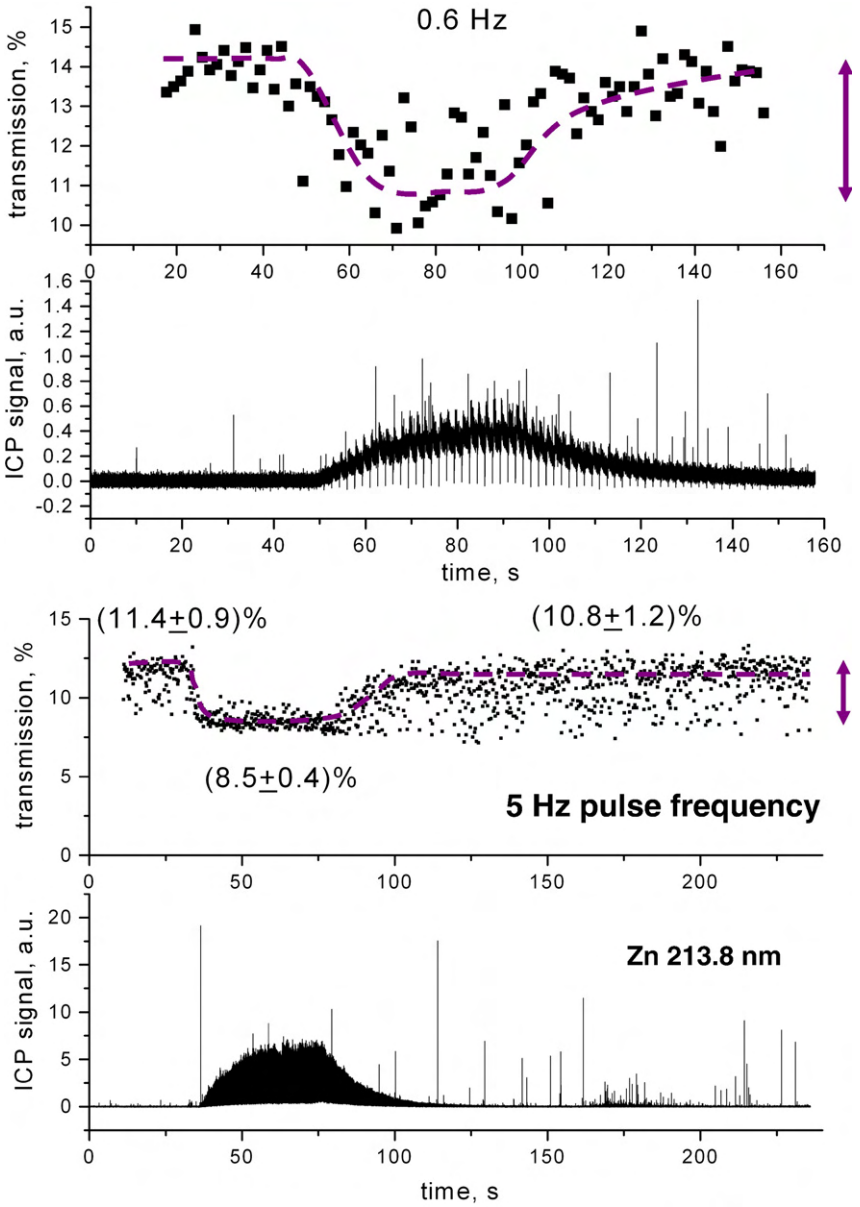

Fig. 4. The transmission of the pre-pulse laser without and with ablation of brass and the corresponding ICP-OES signal of the 213.8 nm Zn line in dependence on time. Ablation started at 45 s and 35 s and stopped at 95 s and 80 s at 0.6 and 5 Hz laser pulse frequency, respectively. The long ICP-OES signals represent the low particle washout of the ablation cell. The spikes in the ICP response are due to larger particles (see also [18]).

increased again slowly as the particles were washed-out of the cell. When increasing the laser frequency to 5 Hz, the transmission was reduced during ablation as with the lower repetition rate. However, the shot-to-shot scatter in the data was smaller than in the 0.6 Hz experiment. This can also be seen in Fig. 5, which shows a histogram of the transmission data presented in the lower part of Fig. 4 (5 Hz pulse frequency). The narrowest distribution was found during ablation when the particle number density in the ablation cell and also the probability of laser-particle interaction was highest. Before and after ablation, the probability of laser-particle interaction was smaller and, therefore, events with transmissions below ~10% were rare.

Overall, one expects an increase in shot-to-shot variability when moving from a pure gas breakdown (i.e. no particles at all) to a gas with particles. However, when moving from a smaller number of particles (i.e. 0.6 Hz) to a greater number of particles at 5 Hz, the statistics actually improve, in that the probability of laser-particle interactions increases from a more chaotic process to a more predictable (i.e. high likelihood) process.

Fig. 6 presents transmission measurements at 5 Hz in air without gas flow (i.e. static chamber). The transmission was about 10.3% before the ablation laser was turned on. The RSD of the transmission data was about 5%. The presence of brass particles during ablation reduced the average transmission from 10.3% to 8.4%, with a much larger scatter than it was observed with gas flow. After the ablation laser was turned off, due to the missing particle wash-out the recovery of the average transmission signal to the value before ablation took much longer than with gas flow.

The interaction of laser-induced plasmas with aerosol particles has been previously explored for both single-pulse [6,21] and dual-pulse LIBS [7], revealing rather complex behavior. Clearly the statistics of shot-to-shot transmission in the static cell reveal considerable variation, including some relatively low transmission events (i.e., increased absorption) after the ablation laser was turned off, which are attributed to laser-particle interactions combined with potential effects of particle-shockwave interactions and changing particle size distributions due to settling of larger particles.

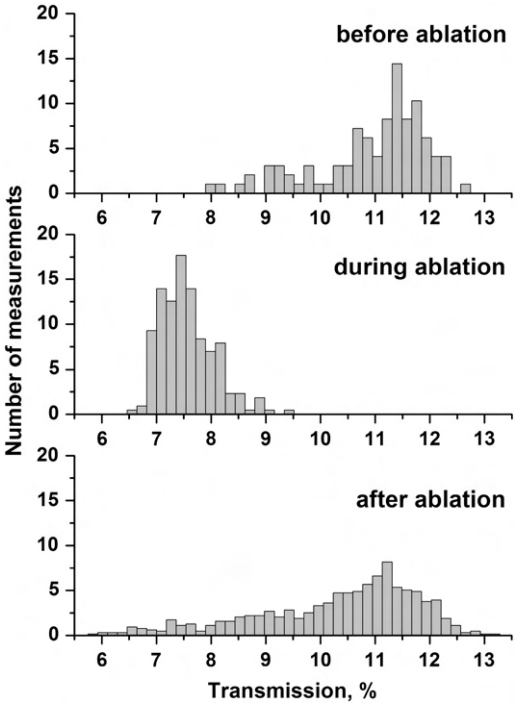

Fig. 5. Evaluation of the transmission measurements with 5 Hz laser pulse frequency displayed in the lower part of Fig. 5.

Complementary results to the laser-particle interaction in the cell were obtained using the second laser platform for breakdown in the pure gas and aerosol systems for more specified aerosol loadings. Table 1 shows the statistics for breakdown in the purified nitrogen, and for breakdown in the two aerosol size distributions, including the

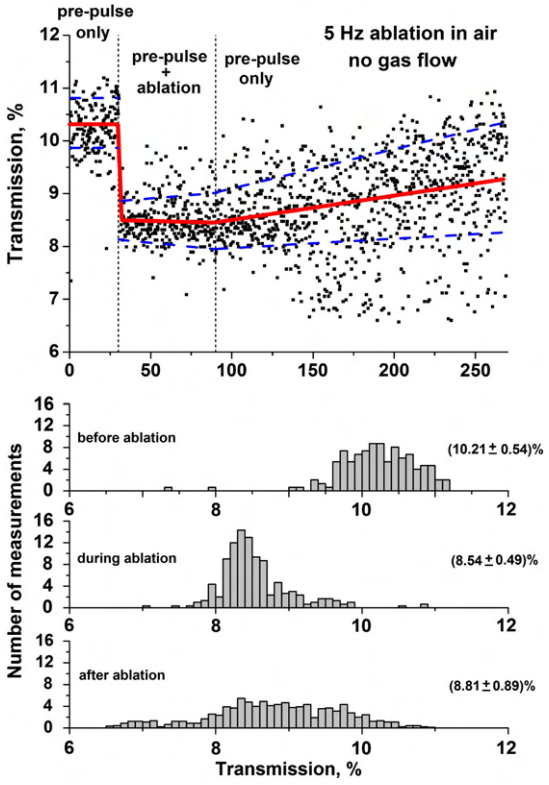

Fig. 6. (Top) transmission of the pre-pulse laser without and with mass ablation from the second laser in air without gas flow through the ablation cell. (bottom) evaluation of the transmission data before, during, and after ablation.

Table 1
Statistics of plasma absorptivity recorded for the single laser experiments in the aerosol chamber for pure nitrogen breakdown and breakdown in the presence of the two aerosol loadings.

	Plasma absorptivity			RSD
	Average	Maximum	Minimum	
Pure nitrogen	0.78	0.81	0.74	4.9%
Aerosol 1	0.82	0.90	0.77	19.8%
Aerosol 2	0.84	0.91	0.76	25.8%

percentage of laser energy coupled into the plasma (correcting for both window optics and aerosol transmission), the maximum and minimum absorption, and the relative standard deviation (RSD). Aerosol 1 corresponds to the 50-nm geometric mean particle size and a total particle loading of about 6000 cm^{-3}, and Aerosol 2 corresponds to the 75-nm geometric mean particle size and a total particle loading of about 9000 cm^{-3}. Under these particle loadings, the probability for direct laser-particle interaction is calculated as 99.92% and 99.99%, respectively, using Poisson sampling statistics and typical plasma parameters [22].

Several important observations are noted under these two aerosol conditions. First, the amount of energy coupled into the laser-induced plasma is increased by about 10% as compared to the pure gas breakdown (i.e. 82–84% absorption vs. 78% absorption). In consideration of the probability of direct laser-particle contact, one can conclude that the presence of aerosol particles triggers the on-set of breakdown forward in the temporal pulse profile, allowing more energy to couple into the plasma. We quantify this below. However, increased absorption via particle interactions brings a significant increase in variability, as the RSD is increased 4- to 5-fold, namely, from the 4.9% value in pure nitrogen (i.e. particle free) to 19.8% and 25.8% for the two aerosol loadings. Clearly the spatial and temporal variability of laser-particle interactions affects the dynamics of plasma initiation. In contrast, the breakdown of the pure gas is a much more predictable event. We note here that a direct measurement of the laser output pulse-to-pulse variation in the absence of any breakdown (with focusing lens removed) shows an RSD of 2.5%; hence, the variable of the nitrogen breakdown is comparable to the variation of the actual laser output.

In Fig. 7, we show the transmitted laser pulse waveforms for pure gas breakdown and for the 75 nm aerosol loading, as well as the incident laser waveform. The transmitted waveforms are consistent with our comments above, that is, the on-set of plasma formation, as determined by the departure from the incident waveform trace, is shifted forward in time by about 1.7 ns under aerosol conditions, allowing more energy to be absorbed into the plasma. Note that even

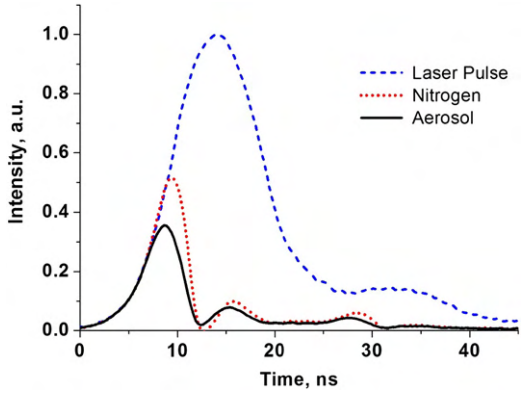

Fig. 7. Incident laser waveform (i.e., no breakdown) along with the transmitted laser waveforms recorded for pure nitrogen breakdown and for breakdown in the 75 nm mean diameter aerosol. Each waveform corresponds to the average of 100 shots, and all waveforms have the same intensity scale.

the positions where the LIBS plasmas with and without aerosol become opaque and partly transparent again for the laser pulse at about 12.5 ns and 16 ns, respectively, are weakly dependent on the presence of particles. This all is clearly the result of direct laser-particle interactions altering the breakdown threshold and plasma dynamics.

Overall, the above data presents a clear picture of the influence of particles on laser-induced breakdown, namely via statistical fluctuations in laser-plasma absorption and transmission, and the subsequent influence on laser ablation via changes in the resulting ICP-OES signals. In the concluding section, we discuss the overall implications for quantitative analysis.

4. Conclusions

4.1. Implications for LIBS and LA-ICP spectrometry

The presence of particles and their influence on the statistics of the measured analyte signal and on the ablation process itself is a general fact which has not only to be considered with single and dual-pulse orthogonal LIBS arrangements, but in *all experimental arrangements where lasers are applied for solid sampling* (i.e., laser ablation). These effects can only be mitigated if the particles are removed from the volume above the laser crater before the next laser shot hits the sample. This can be achieved if laser ablation cells with short wash-out time are applied (see, e.g., [8,23,24]). Laser sampling outside of an ablation cell, such as LIBS at atmospheric conditions, requires, for example, the use of gas nozzle with sufficiently high gas flow to blow the particles out of the focussed region of the laser. However, for actual particle analysis of an aerosol sample, one must consider the implications of plasma-particle interactions [21]. It has to be noted that the influence of particles on the ablation process, as well as the measures for removing them were already discussed recently in [8].

4.2. Single-pulse and double-pulse LIBS

A strong scatter of line intensities in LIBS at very low pulse frequency is an indicator of occasional presence of particles in the focus region if the sample is homogeneous and the laser power is constant from shot-to-shot. Higher pulse frequencies increase the particle number density in the particle-laser interaction volume near the sample surface and reduce the intensity scatter for high sample rates. However, the improved statistics are at the expense of increased plasma shielding, and likely a change of material propagation after a particle seeded breakdown in gas just above the laser crater, due to the particle induced shock-waves.

The effect of particle induced plasma shielding and shock-wave is expected be more pronounced in collinear dual-pulse LIBS [7,15,25] where the breakdown induced by the first laser shot generates a bubble of low gas particle density within the shock-wave, and thereby enabling the ablation of more mass and better atomization and excitation conditions of the analytes with the second shot than without collinear pre-pulse. One can imagine that not only particles from preceding shots may influence the ablation process of the second laser, but also the sampled mass from the first shot which can interact with the second pulse inducing a breakdown above the sample.

4.3. Laser ablation ICP-MS/OES

In LA-ICP spectrometry the particles produced in the ablation process should be transported without loss to the ICP, where they are atomized again and the line emission from the atoms/ions (OES) or the element ions (MS) are measured. Accurate analyzes can only be expected if ***all*** particles produced during ablation are transported without significant loss to the ICP. This condition is fulfilled if the total mass removed is found in particles which are not smaller than ~5 nm and larger than ~1 μm [8,23,24] to avoid losses during the transport by diffusion and inertial settlement, respectively. A plasma breakdown in the gas above the position of laser sampling due to the presence of particles would not only change the laser fluence on the sample and downgrade the statistics of mass removal if the particle number density is very low, e.g., at low laser pulse frequency, but may again change the mass expansion as discussion in [8,26]. The worst scenario would be if particle breakdown gives rise to particle deposition [8].

Acknowledgements

The authors thank the referees of the manuscript for very helpful comments and acknowledge gratefully the financial support for the project “Solving the plasma-analyte interaction problem: Toward a fundamental advancement in plasma-assisted microanalysis and materials characterization” by the National Science Foundation (CHE-0822469) and the Deutsche Forschungsgemeinschaft (Ni 185/38). A part of the experiments was carried out at ISAS in Dortmund (Germany).

References

[1] D.W. Lencioni, Effect of dust on 10.6-μm laser-induced air breakdown, Appl. Phys. Lett. 23 (1973) 12–14.
[2] D.C. Smith, Gas-breakdown initiated by laser-radiation interaction with aerosols and solid-surfaces, J. Appl. Phys. 48 (1977) 2217–2225.
[3] G.H. Canavan, P.E. Nielsen, Focal spot size dependence of gas breakdown induced by particulate ionization, Appl. Phys. Lett. 22 (1973) 409–410.
[4] D.E. Poulain, D.R. Alexander, J.P. Barton, J. Zhang, Interactions of intense ultraviolet-laser radiation with solid aerosols, J. Appl. Phys. 67 (1990) 2283–2288.
[5] G.M. Weyl, Physics of laser-induced breakdown, in: L.J. Radziemski, D.A. Cremers (Eds.), Ch. 1 in Laser-induced Plasmas and Applications, Marcel Dekker, New York, 1989.
[6] V. Hohreiter, A. Ball, D.W. Hahn, Effects of aerosols and laser cavity seeding on spectral and temporal stability of laser-induced plasmas: applications to LIBS, J. Anal. At. Spectrom. 19 (2004) 1289–1294.
[7] B.C. Windom, P.K. Diwakar, D.W. Hahn, Dual-pulse LIBS for analysis of gaseous and aerosol systems: plasma-analyte interactions, Spectrochim. Acta Part B 61 (2006) 788–796.
[8] C.C. Garcia, H. Lindner, K. Niemax, Laser ablation inductively coupled plasma mass spectrometry — current shortcomings, practical suggestions for improving performance, and experiments to guide future development, J. Anal. At. Spectrom. 24 (2009) 14–26.
[9] D.N. Stratis, K.L. Eland, S.M. Angel, Dual-pulse LIBS using a pre-ablation spark for enhanced ablation and emission, Appl. Spectrosc. 54 (2000) 1270–1274.
[10] D.N. Stratis, K.L. Eland, S.M. Angel, Enhancement of aluminium, titanium, and iron in glass using pre-ablation spark dual-pulse LIBS, Appl. Spectrosc. 54 (2000) 1719–1726.
[11] D.N. Stratis, K.L. Eland, S.M. Angel, Effect of pulse delay on a pre-ablation dual-pulse LIBS plasma, Appl. Spectrosc. (2001) 1297–1303.
[12] C. Gautier, P. Fichet, D. Menut, J.L. Lacour, D. L'Hermite, J. Dubessy, Study of the double-pulse setup with an orthogonal beam geometry for laser-induced breakdown spectroscopy, Spectrochim. Acta Part B 60 (2005) 265–275.
[13] C. Gautier, P. Fichet, D. Menut, J.L. Lacour, D. L'Hermite, J. Dubessy, Quantification of the intensity enhancements for the double-pulse laser-induced breakdown spectroscopy in the orthogonal beam geometry, Spectrochim. Acta Part B 60 (2005) 265–275.
[14] H. Lindner, J. Koch, K. Niemax, Production of ultrafine particles by nanosecond laser sampling using orthogonal prepulse laser breakdown, Anal. Chem. 77 (2005) 7528–7533.
[15] J. Scaffidi, S.M. Angel, D.A. Cremers, Emission enhancement mechanisms in dual-pulse LIBS, Anal. Chem. 78 (2006) 24–32.
[16] G. Cristoforetti, S. Legnaioli, L. Pardini, V. Palleschi, A. Salvetti, E. Tognoni, Spectroscopic and shadowgraphic analysis of laser induced plasmas in the orthogonal double pulse pre-ablation configuration, Spectrochim. Acta Part B 61 (2006) 340–350.
[17] G. Cristoforetti, Orthogonal double-pulse versus single-pulse laser ablation at different air pressures: a comparison of the mass removal mechanism, Spectrochim. Acta Part B 64 (2009) 26–34.
[18] M. Miclea, C.C. Garcia, I. Exius, H. Lindner, K. Niemax, Emission spectroscopic monitoring of particle composition, size and transport in laser ablation inductively coupled plasma spectrometry, Spectrochim. Acta Part B 61 (2006) 361–367.
[19] F. Leis, W. Sdorra, J.B. Ko, K. Niemax, Basic investigations for laser microanalysis: I. Optical emission spectrometry of laser produced sample plumes, Mikrochim. Acta II (1989) 185–199.
[20] W. Sdorra, K. Niemax, Basic investigations for laser microanalysis: III. Application of different buffer gases for laser produced sample plumes, Mikrochim. Acta 107 (1992) 319–327.

[21] V. Hohreiter, D.W. Hahn, Plasma-particle interactions in a laser-induced plasma: Implications for laser-induced breakdown spectroscopy, Anal. Chem. 78 (2006) 1509–1514.
[22] J.E. Carranza, D.W. Hahn, Plasma volume considerations for analysis of gaseous and aerosol samples using laser induced breakdown spectroscopy, J. Anal. At. Spectrom. 17 (2002) 1534–1539.
[23] C.C. Garcia, H. Lindner, K. Niemax, Transport efficiency in femtosecond laser ablation inductively coupled plasma mass spectrometry applying ablation cells with short and long washout times, Spectrochim. Acta Part B 62 (2007) 13–19.
[24] H. Lindner, D. Autrique, C.C. Garcia, A. Bogearts, K. Niemax, Optimized transport setup for high repetition rate pulse-separated analysis in laser ablation inductively coupled plasma mass spectrometry, Anal. Chem. 81 (2009) 4241–4248.
[25] M. Corsi, G. Cristoforetti, M. Giuffrida, M. Hildago, S. Legnaioli, V. Palleschi, A. Salvetti, E. Tognoni, C. Vallebona, Three-dimensional analysis of laser-induced plasmas in single and double pulse configuration, Spectrochim. Acta Part B 59 (2004) 723–735.
[26] J. Koch, S. Schlamp, T. Rösgen, D. Fliegel, D. Günther, Visualization of aerosol particles generated by near infrared nano- and femtosecond laser ablation, Spectrochim. Acta Part B 62 (2007) 20–29.